

Development of Thermal Fatigue Testing System and Preliminary Testing

Su Yeong Lee¹, Jin Weon Kim^{2†}, Tae Soon Kim³ and Hun Suk Nam⁴

¹Ph. D Student, Chosun University, Gwangju, Republic of Korea

^{2†}Professor, Chosun University, Gwangju, Republic of Korea (jwkim@chosun.ac.kr)

³Senior Researcher, Central Research Institute, KHNP Co., Daejeon, Republic of Korea

⁴Senior Researcher, Central Research Institute, KHNP Co., Daejeon, Republic of Korea

ABSTRACT

This paper developed a testing system to perform thermal fatigue tests on cylindrical specimens simulating pipe and nozzle joints in nuclear power plants (NPPs) and performed preliminary fatigue tests. The test system generated thermal stresses in the specimen by continuously heating the outer surface while periodically cooling the inner surface. The specimen was heated uniformly by an induction heater and cooled periodically by flowing coolant into the specimen. The cooling time and reheat interval were determined by controlling the timing and sequence of the solenoid valves installed in the cooling system. The preliminary tests confirmed that the simulated specimens with non-uniform external shape were heated uniformly and that a significant temperature gradient across the specimen wall changed during the cooling and reheating. It was also found that under purely thermal cyclic conditions, both axial and circumferential cracks were initiated in the inner surface of the specimen. Axial cracking was dominant and occurred mainly in the thicker sections, with a few circumferential cracks observed in the thinner sections.

INTRODUCTION

Systems, structures, and components (SSCs) of nuclear power plants (NPPs) are subjected to various cyclic loads during operation. They are designed in accordance with the fatigue assessment methods of the design codes and have sufficient margin against fatigue damage (ASME (2019)). As the design codes are known to be overly conservative, a number of studies have proposed alternative assessment methods that are less conservative (ASME BPVC CC N-779 (2003), ASME BPVC CC N-904 (2020), and Asada, S. et al. (2004)). More recently, best-estimate fatigue assessment methods based on elastic-plastic finite element analysis have also been proposed (Jong-Sung Kim. et al. (2020)). However, the proposed methods have not been sufficiently validated with experimental data due to the lack of fatigue test data. In particular, there is limited data available from fatigue tests on specimens that simulate the thermal transient conditions of SSCs induced by internal fluid flow. Therefore, this study developed a thermal fatigue test system capable of simulating the fatigue failure of pipe and nozzle joints in NPPs due to thermal transients, and conducted preliminary tests to confirm the developed test system.

DEVELOPMENT OF A THERMAL FATIGUE TESTING SYSTEM

Design of testing system

Pipe and nozzle joints are known to be cyclically stressed due to periodic temperature changes of the fluids flowing within them and are considered to be a key location for fatigue assessment in the design of NPPs. In this study, a thermal fatigue test system was designed to simulate fatigue damage of pipe and nozzle joints. That is, the specimen was considered to be cylindrical with a non-uniform external shape, and the test system was designed to generate thermal stress by uniformly heating the specimen and periodically cooling the internal surface. The system was also designed to apply mechanical stress to the specimen, in addition to thermal stress. Figure 1 is a schematic diagram of the designed test system.

Division IX (include assigned division number from I to XII and remove this blue explanation text)

As illustrated in Fig. 1, the thermal fatigue test system consists of a loading frame, a heating and cooling systems, and a control and data acquisition (DAQ) system. The loading frame fixes the specimen and applies mechanical loads to the specimen. The specimen is held by the lower and upper fixtures of the loading frame. A load-cell is mounted to the lower fixture to measure axial load applied to the specimen. The upper fixture allows free axial movement during thermal cycling. It also applies monotonic and cyclic axial loads by applying dead weight and constraint, respectively. The specimen is uniformly heated by an induction coil and the heating rate can be adjusted by controlling the heating current of the induction heater. The cooling system supplying coolant to the specimen is a closed-loop system consisting of a water reservoir, circulating pump, and solenoid valves. The coolant temperature is maintained by using a chiller connected to the water reservoir. The flow rate of coolant to the specimen is adjusted by controlling the circulation pump. The solenoid valves control the flow path and flow time, thereby controlling the cooling and reheating times of the specimen. The solenoid valves are controlled by a specially designed controller and temperatures at various locations and load are measured by using a DAQ system.

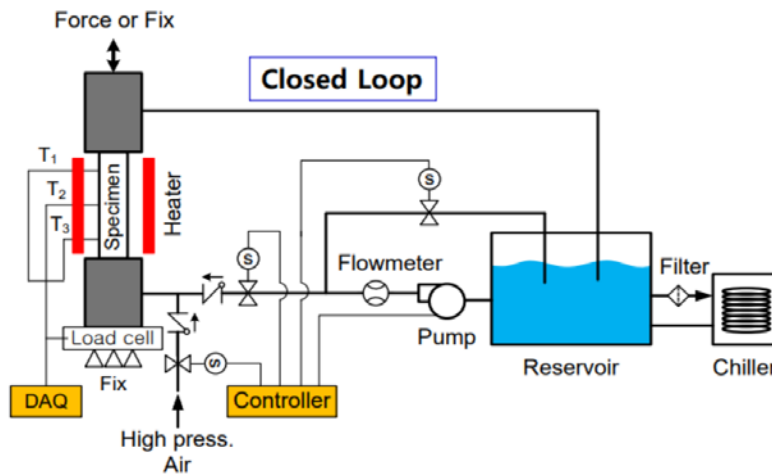


Figure 1. Schematic diagram of the thermal fatigue testing system

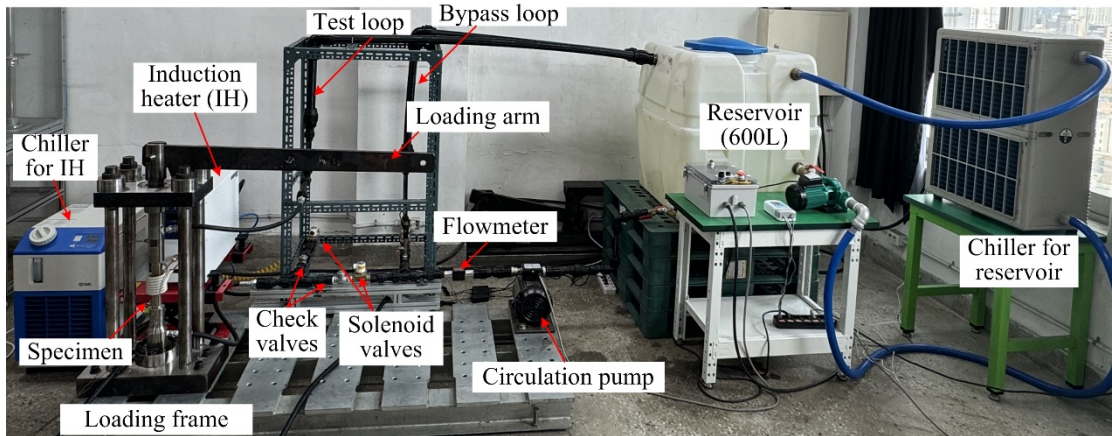
Loading frame

A thermal fatigue test system was constructed based on the conceptual design shown in Fig. 1. Figure 2(a) shows the constructed thermal fatigue test system. As shown in Fig. 2(b), the loading frame consists of fixtures that clamp the specimen and supply cooling water to the specimen, and supports to which the fixtures are connected. Coolant flows into the centre of the lower fixture and out through the specimen to the upper fixture. A load cell with a capacity of 200 kN was mounted on the lower fixture to measure the axial load applied to the specimen.

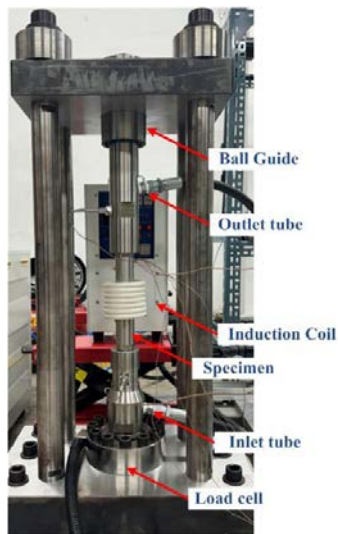
The upper fixture and support have been designed to perform the thermal fatigue test under thermal load only (no mechanical load) and combined thermal and mechanical loads (cyclic and monotonic loads). Thus, the axial load due to friction between the fixture and the support plate has been minimized by the installation of a ball guide. The constraint on the axial movement of the specimen was controlled by a nut at the top, allowing the specimen to be subjected to axial cyclic loading combined with thermal loading during heating and cooling. A loading arm and dead weight were used to apply a constant axial load to the specimen together with thermal loading. Figures 3(a) and (b) present the cyclic and monotonic axial loads applied to the dummy specimen during heating and cooling by restricting axial movement and applying a dead weight, respectively. It has been shown that the fatigue test system is capable of applying cyclic and monotonic loads in the axial direction together with a thermal load.

Heating and cooling systems

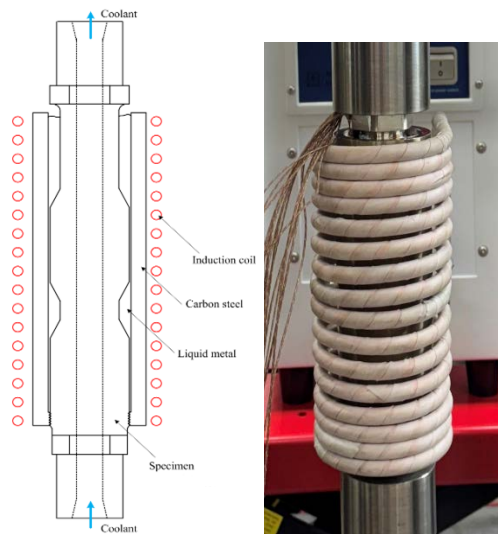
The test system generates thermal stresses in the specimen by continuously heating the outer surface while periodically cooling the inner surface. The specimen was heated uniformly by an induction heater and cooled periodically by flowing coolant into the specimen. The induction heater has an output power of 25 kW and operates at mid-frequency (30 kHz to 80 kHz), and the heating current can be adjusted from 200 A to 1000 A. The heating time to reach a constant temperature depends on the intensity of the heating current, so the heating rate of the specimen is controlled by adjusting the heating current of the induction heater. To uniformly heat a simulated specimen with non-uniform shape, the specimen is placed in a metal cover filled with liquid metal and the outer surface of the metal cover is heated by an induction coil as shown in Fig. 2(c).



(a) Overall system configuration



(b) Loading frame



(c) Heating method for simulated specimen

Figure 2. Photo of the thermal fatigue test system

The cooling system to supply coolant to the specimen consists of a water reservoir, a circulating pump, a flow meter, and a closed-loop with a solenoid valve to control the flow path and time (Figure 2(a)). A chiller is also installed to maintain the coolant at a constant temperature. High pressure air is supplied to dry the inside of the specimen after coolant injection. The coolant flow time and interval and the air flow time are controlled by controlling the opening and closing time of the solenoid valve, and the coolant flow

Division IX *(include assigned division number from I to XII and remove this blue explanation text)*

rate is controlled by a flow regulator installed on the pump. The maximum flow rate of the coolant was measured to be 45.4 L/min and the heat transfer coefficient (h) on the inner surface of the specimen at a flow rate of 45.4 L/min, calculated using the Gnielinski correlation equation (Dewitt D.P.(2006)), is $22.5 \text{ kW/m}^2\text{K}$.

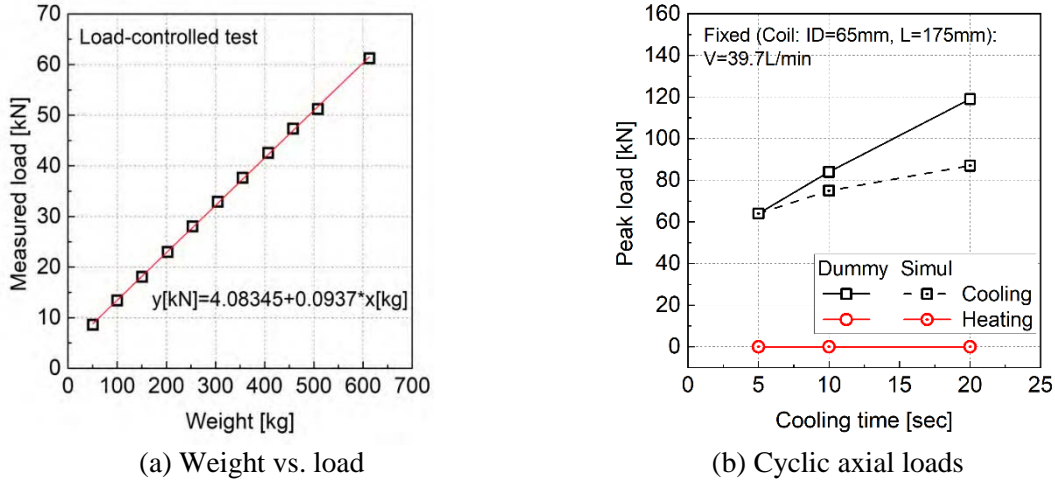


Figure 3. Application of cyclic and constant axial loads by dead weight and displacement constraint

Control and data acquisition system

NI's cDAQ board was used as the control and data acquisition system to control the solenoid valves and to record data. The software for valve control and data acquisition was programmed in LabVIEW. The solenoid valves were controlled sequentially according to the time setting in the on/off method, and the data acquisition interval was programmed so that the user can set the time arbitrarily.

PRELIMINARY TESTING USING SIMULATED SPECIMENS

Simulated specimen and test conditions

In the preliminary test, a cylindrical type specimen with a non-uniform outer diameter was used to simulate the pipe and nozzle joints in the NPPs. The simulated specimen has a constant inner diameter of 13 mm and two different outer diameters (29 mm and 39 mm). It also has a notched section with a smaller diameter. Detailed dimensions of the specimen are shown in Fig. 4.

In order to confirm the performance of the developed fatigue test system, the preliminary tests were carried out using a simulated specimen. The tests were conducted under the conditions of a heating current of 500A, a coolant flow rate of 39.7L/min ($h=20 \text{ kW/m}^2\text{K}$), and a surface temperature of $350 \text{ }^\circ\text{C}$. The cooling and reheating times were 5 and 56 seconds, respectively.

Temperature distributions and gradients

The temperature distributions in the longitudinal and thickness directions during cooling and heating were investigated in preliminary tests. The longitudinal temperature distribution was determined from the temperatures along the length of the specimen, which were measured by the thermocouples welded to the outer surface during cooling and heating. Figure 5 shows the temperatures measured during heating and cooling as a function of longitudinal location. The temperature during cooling is not uniform, but during heating it is almost uniform along the length of the specimen, except at both ends of the specimen. The non-

Division IX *(include assigned division number from I to XII and remove this blue explanation text)*

uniform temperature distribution during cooling is due to thinner sections of the specimen cooling faster than thicker sections. Thus, it is seen that the test system is able to heat the specimen with non-uniform outer diameter uniformly.

The temperature distribution along the thickness of the specimen was determined by measuring the temperature at different locations along the thickness direction during heating and cooling. To measure the temperature at different locations, holes of different depths were machined in the wall of the specimen and thermocouples were mounted. The location and depth of the holes are shown in Figure 6(a). Figure 6(b) presents the temperature distribution along the thickness during heating and cooling. It shows that during heating, the temperatures within the wall of the specimen are almost the same regardless of the specimen thickness. However, during cooling, the temperature near the inner surface drops considerably while the temperature of the outer surface remains the same. Eventually, a large temperature gradient is formed in the thickness direction. As the heating and cooling is repeated, the temperature gradient in the wall of the sample changes significantly, and the significant change in temperature gradient generates the cyclic stresses in the circumferential and longitudinal directions.

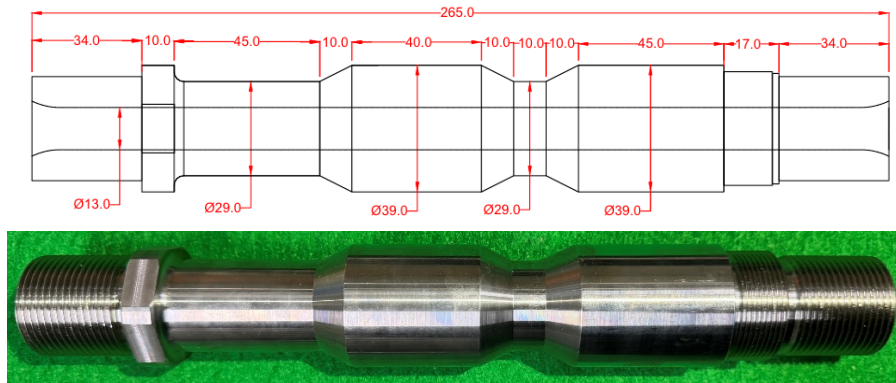


Figure 4. Geometry of simulated specimen

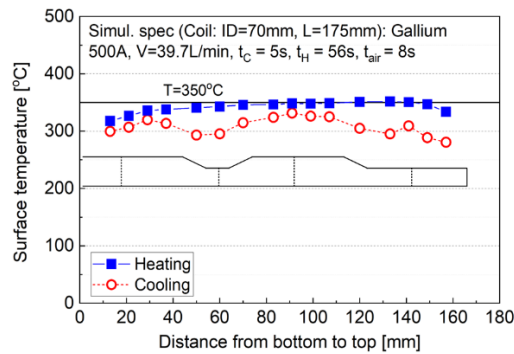
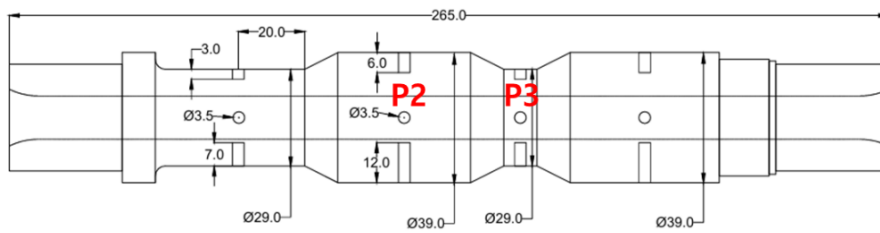
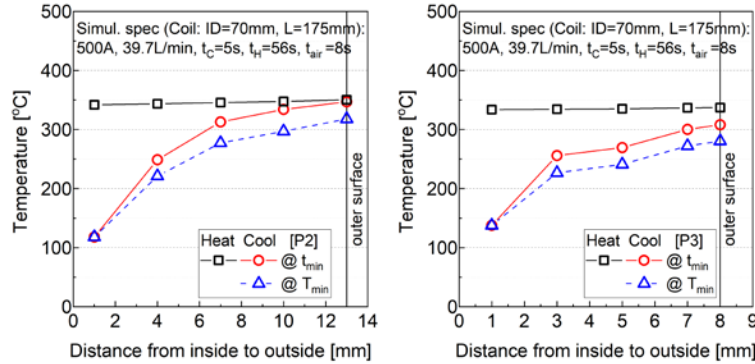


Figure 5. Longitudinal distribution of temperature in the simulated sample



(a) Location and depth of the holes

Division IX (include assigned division number from I to XII and remove this blue explanation text)



(b) Temperature gradient in the thickness direction

Figure 6. Temperature gradient in the thickness direction of the simulated specimen

Fatigue cracking

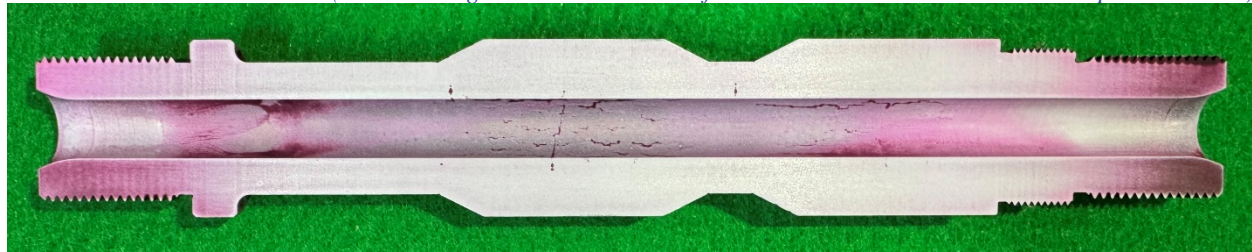
In the above section, it can be seen that the developed test system is able to heat the simulated specimen uniformly and produces a significant temperature gradient in the wall of the specimen. Using this test system, a thermal fatigue tests were carried out under unconstrained conditions, i.e., free axial movement. During testing, the temperature of the specimen was monitored using 14 thermocouples welded to the specimen surface to ensure proper heating and cooling of the specimen. The coolant temperature at the inlet and outlet was also monitored. The test was periodically interrupted and the internal surface was inspected using an endoscope camera to determine the crack initiation and propagation.

Figure 7 shows the photographs taken by endoscope of the inner surface after 10,000, 15,000 and 30,000 thermal cycles. At 10,000 cycles, evidence of crack initiation in the axial direction was observed in the thicker section (P2 in Fig. 6(a)). At 15,000 cycles, evidence of circumferential cracking was also observed in the thinner section (P3 in Fig. 6(a)). Figure 6(c), taken after 30,000 cycles exhibits that a number of axial and circumferential cracks had formed and that the length of the cracks had increased. The test was terminated at 30,000 cycles and the specimen was cut open to perform a liquid penetrant test (PT) on the internal surface to examine the crack pattern and length and depth. The PT examination in the longitudinal section (Fig. 8(a)) shows that the numerous axial cracks have grown in the thicker sections and several circumferential cracks have grown in the notched and transition sections. The circumferential section also shows that the numerous axial cracks started at inner surface and propagated outwards and that the maximum depth of the axial cracks exceeded 3.5mm (see Fig. 8(b)). Therefore, it is confirmed that the thermal fatigue damage induced by thermally transient fluid flow in pipe and nozzle joints can be simulated using the developed test system and specimen.

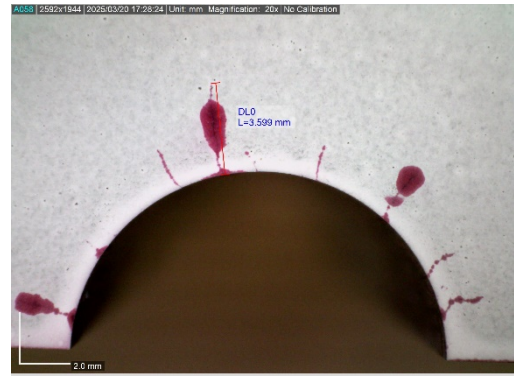
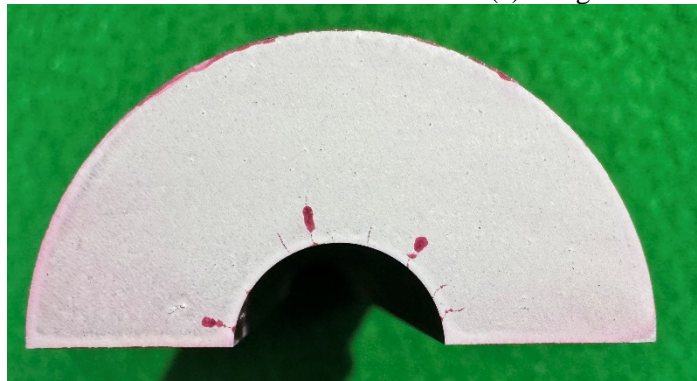


(a) 10,000 cycles (thicker section) (b) 15,000 cycles (thinner section) (c) 30,000 cycles (thicker section)

Figure 7. Photographs taken from the inside of the specimen



(a) Longitudinal section



(b) Circumferential section

Figure 8. Results of liquid penetrant test

CONCLUSIONS

This study developed a thermal fatigue test system and conducted preliminary test using simulated specimens. The following conclusions were drawn from the results;

- 1) The developed test system was able to heat the specimen with non-uniform outer diameter uniformly. In addition, a large temperature gradient was formed in the thickness direction and the temperature gradient changed significantly with repeated heating and cooling.
- 2) The numerous axial cracks grew in the thicker sections of the specimen and several circumferential cracks grew in the notched and transition sections. The cracks started at inner surface and propagated outwards.
- 3) The thermal fatigue damage induced by thermally transient fluid flow in pipe and nozzle joints can be simulated using the developed test system and specimen.

Acknowledgement

This work was supported by KOREA HYDRO & NUCLEAR POWER CO., LTD (No. 2023-Technology-05)

REFERENCES

- ASME. (2019). "ASME Boiler and Pressure Vessels Code Sec. III: Rule for Construction of Nuclear Facility Components," *American Society of Mechanical Engineers*, TX.
- ASME BPVC Code Case N-779. (2003). "Alternative Rules for Simplified Elastic-Plastic Analysis," *American Society of Mechanical Engineers*, NY.
- ASME BPVC Code Case N-904. (2020). "Alternative Rules for Simplified Elastic-Plastic Analysis," *American Society of Mechanical Engineers*, NY.

Division IX (*include assigned division number from I to XII and remove this blue explanation text*)

- Asada, S. Okamoto, A. Nishiguchi, I. Aoki, M. and Asada, Y. (2004). “Technical Bases for Alternative Stress Evaluation Criteria in Japan Based on Partial Inelastic Analyses,” *Proc. of ASME 2004 PVP Conference*, CA.
- Dewitt, D.P. Bergman, T.L. Lavine, A.S. and Incropera, F.P. (2006). “Fundamentals of Heat and Mass Transfer, 6th ed,” *John Wiley & Sons*.
- Jong-Sung Kim and Jun-Young Kim. (2020). “Simplified elastic-plastic analysis procedure for strain-based fatigue assessment of nuclear safety class 1 components under severe seismic loads,” *Nuclear Engineering and Technology*, KR, 52 2918-2927.